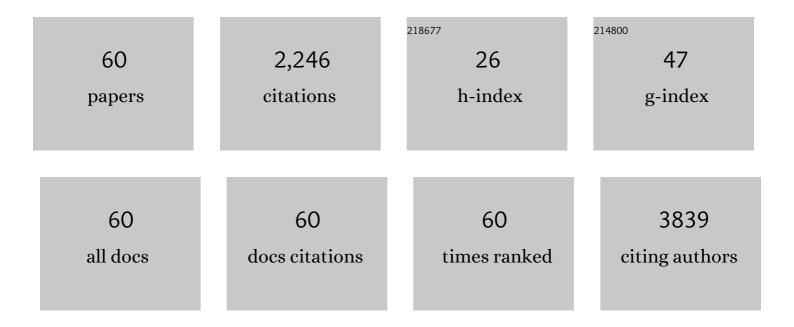
Raul Quesada-Cabrera

List of Publications by Year in descending order

Source: https://exaly.com/author-pdf/5405478/publications.pdf Version: 2024-02-01



#	Article	IF	CITATIONS
1	Facile formation of black titania films using an atmospheric-pressure plasma jet. Green Chemistry, 2022, 24, 2499-2505.	9.0	3
2	Charge Transport Phenomena in Heterojunction Photocatalysts: The WO ₃ /TiO ₂ System as an Archetypical Model. ACS Applied Materials & Interfaces, 2021, 13, 9781-9793.	8.0	24
3	Generating, probing and utilising photo-induced surface oxygen vacancies for trace molecular detection. , 2021, , .		0
4	The Effect of Photoinduced Surface Oxygen Vacancies on the Charge Carrier Dynamics in TiO ₂ Films. Nano Letters, 2021, 21, 8348-8354.	9.1	29
5	Probing the Role of Atomic Defects in Photocatalytic Systems through Photoinduced Enhanced Raman Scattering. ACS Energy Letters, 2021, 6, 4273-4281.	17.4	22
6	Qualitative Approaches Towards Useful Photocatalytic Materials. Frontiers in Chemistry, 2020, 8, 817.	3.6	5
7	Patterning of metal oxide thin films using a H ₂ /He atmospheric pressure plasma jet. Green Chemistry, 2020, 22, 1406-1413.	9.0	15
8	Dynamics of Photoâ€Induced Surface Oxygen Vacancies in Metalâ€Oxide Semiconductors Studied Under Ambient Conditions. Advanced Science, 2019, 6, 1901841.	11.2	62
9	High Defect Nanoscale ZnO Films with Polar Facets for Enhanced Photocatalytic Performance. ACS Applied Nano Materials, 2019, 2, 2881-2889.	5.0	29
10	Surface Oxygen Vacancies: Dynamics of Photoâ€Induced Surface Oxygen Vacancies in Metalâ€Oxide Semiconductors Studied Under Ambient Conditions (Adv. Sci. 22/2019). Advanced Science, 2019, 6, 1970132.	11.2	3
11	Photo-induced enhanced Raman spectroscopy (PIERS): sensing atomic-defects, explosives and biomolecules. , 2019, , .		2
12	Deeper Understanding of Interstitial Boron-Doped Anatase Thin Films as A Multifunctional Layer Through Theory and Experiment. Journal of Physical Chemistry C, 2018, 122, 714-726.	3.1	16
13	Direct and continuous hydrothermal flow synthesis of thermochromic phase pure monoclinic VO ₂ nanoparticles. Journal of Materials Chemistry C, 2018, 6, 11731-11739.	5.5	15
14	Photocatalytic and electrically conductive transparent Cl-doped ZnO thin films <i>via</i> aerosol-assisted chemical vapour deposition. Journal of Materials Chemistry A, 2018, 6, 12682-12692.	10.3	34
15	Ultraviolet Radiation Induced Dopant Loss in a TiO ₂ Photocatalyst. ACS Catalysis, 2017, 7, 1485-1490.	11.2	18
16	Photocatalysis: Evidence and Effect of Photogenerated Charge Transfer for Enhanced Photocatalysis in WO ₃ /TiO ₂ Heterojunction Films: A Computational and Experimental Study (Adv. Funct. Mater. 18/2017). Advanced Functional Materials, 2017, 27, .	14.9	1
17	Optimized Atmospheric-Pressure Chemical Vapor Deposition Thermochromic VO ₂ Thin Films for <i>Intelligent</i> Window Applications. ACS Omega, 2017, 2, 1040-1046.	3.5	56
18	Evidence and Effect of Photogenerated Charge Transfer for Enhanced Photocatalysis in WO ₃ /TiO ₂ Heterojunction Films: A Computational and Experimental Study. Advanced Functional Materials, 2017, 27, 1605413.	14.9	115

#	Article	IF	CITATIONS
19	Sensitive and specific detection of explosives in solution and vapour by surface-enhanced Raman spectroscopy on silver nanocubes. Nanoscale, 2017, 9, 16459-16466.	5.6	78
20	Nanoscale, conformal films of graphitic carbon nitride deposited at room temperature: a method for construction of heterojunction devices. Nanoscale, 2017, 9, 16586-16590.	5.6	20
21	Qualitative XANES and XPS Analysis of Substrate Effects in VO ₂ Thin Films: A Route to Improving Chemical Vapor Deposition Synthetic Methods?. Journal of Physical Chemistry C, 2017, 121, 20345-20352.	3.1	22
22	Particle size, morphology and phase transitions in hydrothermally produced VO ₂ (D). New Journal of Chemistry, 2017, 41, 9216-9222.	2.8	26
23	On the apparent visible-light and enhanced UV-light photocatalytic activity of nitrogen-doped TiO 2 thin films. Journal of Photochemistry and Photobiology A: Chemistry, 2017, 333, 49-55.	3.9	29
24	Photo-induced enhanced Raman spectroscopy for universal ultra-trace detection of explosives, pollutants and biomolecules. Nature Communications, 2016, 7, 12189.	12.8	201
25	Scalable Production of Thermochromic Nb-Doped VO ₂ Nanomaterials Using Continuous Hydrothermal Flow Synthesis. Journal of Nanoscience and Nanotechnology, 2016, 16, 10104-10111.	0.9	14
26	Where Do Photogenerated Holes Go in Anatase:Rutile TiO ₂ ? A Transient Absorption Spectroscopy Study of Charge Transfer and Lifetime. Journal of Physical Chemistry A, 2016, 120, 715-723.	2.5	128
27	Intelligent Multifunctional VO ₂ /SiO ₂ /TiO ₂ Coatings for Self-Cleaning, Energy-Saving Window Panels. Chemistry of Materials, 2016, 28, 1369-1376.	6.7	221
28	Study of the photocatalytic activity of Pt-modified commercial TiO2 for hydrogen production in the presence of common organic sacrificial agents. Applied Catalysis A: General, 2016, 518, 189-197.	4.3	35
29	Exploring the pressure–temperature behaviour of crystalline and plastic crystalline phases of N-isopropylpropionamide. CrystEngComm, 2015, 17, 2562-2568.	2.6	1
30	High-throughput synthesis of core–shell and multi-shelled materials by fluidised bed chemical vapour deposition. Case study: double-shell rutile–anatase particles. Journal of Materials Chemistry A, 2015, 3, 17241-17247.	10.3	6
31	Silicalite-1/glass fibre substrates for enhancing the photocatalytic activity of TiO2. RSC Advances, 2015, 5, 6970-6975.	3.6	3
32	Multifunctional P-Doped TiO ₂ Films: A New Approach to Self-Cleaning, Transparent Conducting Oxide Materials. Chemistry of Materials, 2015, 27, 3234-3242.	6.7	113
33	Functionalised gold and titania nanoparticles and surfaces for use as antimicrobial coatings. Faraday Discussions, 2014, 175, 273-287.	3.2	16
34	Photocatalytic Evidence of the Rutileâ€ŧoâ€Anatase Electron Transfer in Titania. Advanced Materials Interfaces, 2014, 1, 1400069.	3.7	43
35	A simple, low-cost CVD route to thin films of BiFeO3 for efficient water photo-oxidation. Journal of Materials Chemistry A, 2014, 2, 2922.	10.3	89
36	Critical influence of surface nitrogen species on the activity of N-doped TiO2 thin-films during photodegradation of stearic acid under UV light irradiation. Applied Catalysis B: Environmental, 2014, 160-161, 582-588.	20.2	44

#	Article	IF	CITATIONS
37	Single-step synthesis of doped TiO2 stratified thin-films by atmospheric-pressure chemical vapour deposition. Journal of Materials Chemistry A, 2014, 2, 7082.	10.3	7
38	A simple and low-cost method for the preparation of self-supported TiO ₂ –WO ₃ ceramic heterojunction wafers. Journal of Materials Chemistry A, 2014, 2, 17602-17608.	10.3	19
39	Action spectra of P25 TiO2 and a visible light absorbing, carbon-modified titania in the photocatalytic degradation of stearic acid. Applied Catalysis B: Environmental, 2014, 150-151, 338-344.	20.2	56
40	High-Throughput Continuous Hydrothermal Synthesis of Nanomaterials (Part II): Unveiling the As-Prepared Ce _{<i>x</i>} Zr _{<i>y</i>} Y _{<i>z</i>} O _{2â^î´} Phase Diagram. ACS Combinatorial Science, 2013, 15, 458-463.	3.8	14
41	Scale Up Production of Nanoparticles: Continuous Supercritical Water Synthesis of Ce–Zn Oxides. Industrial & Engineering Chemistry Research, 2013, 52, 5522-5528.	3.7	86
42	Identification of new pillared-layered carbon nitride materials at high pressure. Scientific Reports, 2013, 3, 2122.	3.3	15
43	Photocatalytic activity of needle-like TiO2/WO3â^'x thin films prepared by chemical vapour deposition. Journal of Photochemistry and Photobiology A: Chemistry, 2012, 239, 60-64.	3.9	34
44	A novel route to Pt–Bi2O3 composite thin films and their application in photo-reduction of water. Inorganica Chimica Acta, 2012, 380, 328-335.	2.4	27
45	Spectroscopic studies of sulfite-based polyoxometalates at high temperature and high pressure. Journal of Solid State Chemistry, 2012, 186, 171-176.	2.9	15
46	Structural and Mechanical Properties of TTR105-115 Amyloid Fibrils fromÂCompression Experiments. Biophysical Journal, 2011, 100, 193-197.	0.5	19
47	Polyamorphic Amorphous Silicon at High Pressure: Raman and Spatially Resolved X-ray Scattering and Molecular Dynamics Studies. Journal of Physical Chemistry B, 2011, 115, 14246-14255.	2.6	33
48	Exploring the thermochromism of sulfite-embedded polyoxometalate capsules. Physical Chemistry Chemical Physics, 2011, 13, 7295.	2.8	19
49	Nanomechanical and Structural Properties of Native Cellulose Under Compressive Stress. Biomacromolecules, 2011, 12, 2178-2183.	5.4	57
50	High-pressure synthesis and structural behavior of sodium orthonitrate Na3NO4. Journal of Solid State Chemistry, 2011, 184, 915-920.	2.9	9
51	Pressure-induced phase transitions in <scp>L</scp> -alanine, revisited. Acta Crystallographica Section B: Structural Science, 2010, 66, 458-471.	1.8	73
52	High-Pressure Behavior and Polymorphism of Titanium Oxynitride Phase Ti _{2.85} O ₄ N. Journal of Physical Chemistry C, 2010, 114, 8546-8551.	3.1	8
53	Amorphous X-Ray Diffraction at High Pressure: Polyamorphic Silicon and Amyloid Fibrils. NATO Science for Peace and Security Series B: Physics and Biophysics, 2010, , 469-479.	0.3	1
54	Low temperature/high pressure polymorphism in dl-cysteine. CrystEngComm, 2010, 12, 2551.	2.6	49

#	Article	IF	CITATIONS
55	In situ investigations of the polyoxometalate Trojan Horse compound K7Na[WVI18O56(SO3)2(H2O)2]·20H2O under high temperature and high pressure conditions. CrystEngComm, 2010, 12, 2568.	2.6	7
56	Tetrahedrally bonded dense <mml:math <br="" xmlns:mml="http://www.w3.org/1998/Math/MathML">display="inline"><mml:mrow><mml:msub><mml:mtext>C</mml:mtext><mml:mn>2</mml:mn></mml:msub><m a defective wurtzite structure: X-ray diffraction and Raman scattering results at high pressure and ambient conditions. Physical Review B, 2009, 80, .</m </mml:mrow></mml:math>	ml:msub>	<mml:mtext></mml:mtext>
57	Compressibility of insulin amyloid fibrils determined by X-ray diffraction in a diamond anvil cell. High Pressure Research, 2009, 29, 665-670.	1.2	9
58	Pressure-induced structural transformations of the Zintl phase sodium silicide. Journal of Solid State Chemistry, 2009, 182, 2535-2542.	2.9	12
59	High-pressure x-ray scattering and computer simulation studies of density-induced polyamorphism in silicon. Physical Review B, 2007, 75, .	3.2	87
60	Metastable phase transitions and structural transformations in solid-state materials at high pressure. Phase Transitions, 2007, 80, 1003-1032.	1.3	14